

## An Experimental Study of a Smart Radiator Device for Enhanced Passive Thermal Control of Small Spacecraft

Aimee Carvey, Philip Ferguson  
University of Manitoba  
66 Chancellors Cir, Winnipeg, MB R3T 5V6, Canada; 204-223-6897  
carveya@myumanitoba.ca

Jean-Francois Thibault  
Magellan Aerospace Limited  
400 March Rd, Suite 225, Ottawa, Ontario K2K 2E4; 613-820-1287 x 3915  
Jean-Francois.Thibault@magellan.aero

Emile Haddad  
MPB Communications Inc.  
147 Hymus Blvd, Pointe-Claire, QC H9R 1E9; 514-694-8751  
emile.haddad@mpbc.ca

### ABSTRACT

Small satellites often face thermal control challenges due to their restricted power and low thermal capacitance (leading to wide temperature swings). Smart Radiator Devices (SRDs) provide a spacecraft with improved passive thermal control over traditional radiator materials as their thermal properties change with temperature. SRDs reduce the power consumed by a satellite's thermal control system as they facilitate rapid radiative heat transfer when the spacecraft is hot while suppressing radiation when cold, thereby reducing the heater power required to maintain acceptable temperatures. The SRD emissivity variations also reduce the spacecraft temperature variability due to their tighter thermal control. In this paper, we study the benefits of an SRD that transitions emissivity from low to high at approximately 25°C, increasing its radiative heat transfer and allowing the host spacecraft to cool more quickly. We performed thermal vacuum testing on an SRD mounted to a representative model of a CubeSat panel. We discuss the results of this testing, the lessons learned through this process, and the next steps with this research.

### INTRODUCTION

When designing spacecraft, engineers must consider the challenges of the harsh space environment. Cosmic radiation<sup>1</sup>, orbital disturbances<sup>2</sup>, launch vibration<sup>3</sup>, atomic oxygen<sup>4</sup>, and impacts from orbital debris and micrometeoroids<sup>5</sup> all pose significant difficulties for space systems engineers. One of the greatest difficulties, however, has been designing for the thermal environment of space<sup>6</sup>. Although significant research has gone towards spacecraft thermal design<sup>7,8,9,10</sup>, the continual trend towards higher power and increasingly complicated payloads increase the strain on the thermal control subsystem<sup>11</sup>.

Thermal control is especially challenging for small satellites, an area of space exploration where research interest and spacecraft functionality has been growing exponentially in the past decades<sup>12</sup>. The low mass and small size of small satellites leads to a low thermal mass that makes them prone to rapid temperature swings<sup>13</sup>. In addition to these concerns, small satellites have the added constraint of limited power available to all

subsystems, including thermal<sup>14</sup>. For these reasons, small satellites would benefit from advanced thermal control technologies that improve performance over traditional passive methods. This paper evaluates the potential benefits of an advanced, passive thermal control methodology enabled by Smart Radiator Device (SRD).

### Background

The vacuum of space forces spacecraft to use thermal radiation as the only means of heat transfer external to the spacecraft. Radiative heat transfer obeys the following relationship:

$$Q_{rad} = A\sigma\epsilon F(T_{surface}^4 - T_{ambient}^4) \quad (1)$$

where  $Q_{rad}$  is the heat transfer due to radiation,  $A$  is the area of the radiating surface,  $\sigma$  is the Stefan Boltzmann constant,  $\epsilon$  is the emissivity of the radiating surface,  $F$  is the view factor from the radiating surface to the ambient,  $T_{surface}$  is the temperature of the radiating surface, and  $T_{ambient}$  is the temperature of the surroundings to which

the surface is radiating<sup>6</sup>. In order to control the amount of heat lost to the environment through radiation, satellite designers will often cover the exterior of spacecraft with Multi Layer Insulation (MLI) that has a very low effective emissivity of 0.015 to 0.03<sup>15</sup>.

Throughout the life of a spacecraft, internal and external thermal influences (*i.e.*, solar illumination and varying power demands) can cause temperature fluctuations within the spacecraft<sup>6</sup>. Without adequate thermal regulation, periods of high heat generation can cause the satellite to exceed the thermal requirements of temperature-sensitive components such as electronics and batteries. Therefore, satellites typically incorporate some method of rejecting heat in order to keep units within acceptable thermal conditions during hot situations.

The most commonly used device for cooling satellites is the radiator. The biggest advantages of using radiators for satellite cooling are the low cost and robustness of the design. Compared to active cooling methods such as louvers, the radiator is much lighter and simpler in design<sup>6</sup>. However, the drawback of the radiator is that there is little to no variation in the quantity of heat rejected by the radiator throughout an orbit. This means that whether the satellite is in a period of high or low heat generation, the radiator will be rejecting the same amount of heat.

When designing a spacecraft thermal management system, designers calculate the size of radiators required to reject the correct amount of heat in a worst-case hot situation<sup>6</sup>. This practice is necessary to ensure the radiators will maintain all units below their maximum temperature limits in all load cases, but especially in the hottest scenario. Unfortunately, this means that when the spacecraft enters a period of low heat generation the radiators will reject too much heat, requiring heater power in many low power scenarios. It also means that satellites often experience large temperature swings between sun and eclipse periods. When thermal engineers are designing a spacecraft to meet temperature requirements while minimizing input power, this often results in units operating at the outer edges of their allowable temperature ranges. Thus, the fixed nature of standard radiators leads to significant power and thermal constraints, particularly for small satellites.

### ***Variable Emissivity Radiators***

In order to improve upon the traditional radiator, several<sup>14,16,17</sup> have proposed new designs that provide a method of changing the emissivity, either passively or actively. This variable emissivity enables greater control of radiative heat loss, as the radiator would exhibit low emissivity in low-heat scenarios, and a higher emissivity

in high-heat scenarios<sup>18</sup>. This emissivity control mitigates the fixed-nature challenges of a standard radiator, thereby reducing or even eliminating the need for some heaters and reducing spacecraft temperature swings<sup>17</sup>.

For a variable emissivity radiator, there are three important properties to evaluate the performance of a technology: the maximum emissivity ( $\epsilon_H$ ), the dynamic range in emissivity ( $\Delta\epsilon$ ), and the switching temperature ( $T_s$ ). In order to provide sufficient cooling without large increases in required radiator area,  $\epsilon_H$  should be as close as possible to that of conventional radiators (0.81-0.88), or ideally higher<sup>6</sup>. Dynamic range should be maximized, as this is proportional to the efficiency of the technology; a higher emissivity variation means a more effective radiator. For reference, various louver designs have an effective  $\Delta\epsilon$  of 0.29-0.61<sup>6</sup>. The switching temperature, the temperature where the emissivity of the radiator transitions from low to high, should be somewhere near room temperature in order to maintain the satellite at a comfortable temperature<sup>17</sup>.

One category of variable emissivity radiators requires an active input to switch between the high emissivity and low emissivity states. Some methods of switching emissivity that researchers have suggested include microelectromechanical systems (MEMS)<sup>14,16</sup> and electrostatic charging<sup>19</sup>. A second category of variable emissivity radiators are Smart Radiator Devices, or SRDs. These radiators consist of a passive coating that changes its emissivity in response to temperature changes alone (no power input required). The custom coatings exhibit low emissivity when they are cool and increase their emissivity as their temperature increases, providing passive, variable heat rejection without any power input<sup>20</sup>.

MPB Communications Inc.<sup>20</sup> has developed an SRD made from thin films of VO<sub>2</sub> doped with tungsten. Through their research and manufacturing trials, MPB has demonstrated a combination of desirable thermo-optical properties for SRDs; for instance, with a 2.1% tungsten doping level MPB has produced tiles with  $\Delta\epsilon = 0.43$ , high emissivity of 0.81, and a switching temperature of 31.5°C<sup>17</sup>. This technology shows a significant increase in  $\Delta\epsilon$  over the two active designs, as well as an acceptably high  $\epsilon_H$  and a relatively low switching temperature.

This paper presents an investigation of the performance of a set of MPB SRDs in a characteristic space environment. The composition of these SRDs is similar to those described in reference 17, but not identical. Four separate SRD tiles installed on a single plate comprised the test article. Prior to delivering the SRDs to us for

testing, MPB performed initial testing of the SRDs to determine baseline high and low emissivity values. The four SRDs have slight variations in their measured properties. Due to the small size of the test article and difficulties in instrumenting separate SRDs, we will use average properties of the four SRDs for the purposes of this paper. Table 1 shows the properties as measured by MPB, as well as the calculated averages.

**Table 1: Properties of SRDs used for testing as measured by MPB.**

SRD	$\epsilon_L(@-10^\circ\text{C})$	$\epsilon_H(@100^\circ\text{C})$	$\Delta\epsilon$
1	0.35	0.75	0.40
2	0.34	0.75	0.41
3	0.36	0.76	0.40
4	0.35	0.76	0.41
Average	0.35	0.755	0.405

The evaluation of the SRD performance occurred in two parts: first, by thermal vacuum chamber testing of the SRDs in a flight-representative configuration, and second by analysis of the resulting test data. We will first describe the test configuration and equipment used for testing, before discussing the results.

### THERMAL VACUUM CHAMBER TESTING

The Thermal Vacuum (TVAC) test campaign described in this article is the result of collaboration between four organizations: Magellan Aerospace Limited, MPB Communications, the University of Manitoba (U of M), and Kepler Communications. Magellan Aerospace has been involved with MPB as they developed their SRDs, and have secured an upcoming flight opportunity for the SRDs on a Kepler Communications CubeSat launching in 2019. The SRDs will be the primary thermal control method on the satellite, providing flight heritage for the SRDs in a functioning role. Magellan Aerospace is providing the systems engineering support to Kepler Communications as they integrate the SRDs on to the satellite.

Magellan Aerospace also has a strong working relationship with researchers at the U of M, including joint ownership of the Advanced Satellite Integration Facility at the Magellan plant in Winnipeg. Through this relationship, Magellan is providing U of M researchers with an opportunity to perform testing on the SRD tiles that will be flying on the Kepler Communications satellite. Therefore, the SRDs we tested were bonded to an aluminum interface plate, from here on called the SRD plate, which will become the radiator assembly on the Kepler CubeSat.

The SRD plate is made of machined 6063-T6 aluminum with approximate dimensions of 10 cm x 10 cm x 2 mm. There are four SRD tiles epoxied to one side of the SRD plate (Stycast 2850FT epoxy with Catalyst 9). The opposite side of the SRD plate has four parallel grooves that will interface to a heat pipe on the satellite in order to transfer heat from the payload to the SRDs. The exposed aluminum surfaces on the SRD mounting side of the plate are black anodized, while all other surfaces are untreated aluminum. Figure 1 shows the CAD model of both sides of the SRD plate, with the SRDs shaded in purple on the left.

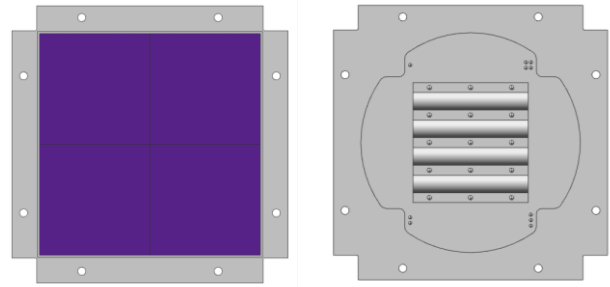


**Figure 1: CAD model of SRD plate- SRD mounting side on left, heat pipe interface side on right.**

MPB performed emissivity testing of the SRDs prior to delivery, but this testing did not occur in a vacuum or mounted to the flight structure. In order to verify the SRD performance in a space-representative environment as well as the emissivity switching profile, we performed testing of the SRDs in a TVAC chamber. The TVAC chamber that we used for testing is located in the smaller Satellite Integration Facility at Magellan Aerospace, which is a class 100,000 clean room. The TVAC chamber has a minimum platen temperature capability of  $-75^\circ\text{C}$  using a methanol coolant. We mounted the SRD plate above the platen so that the SRDs would radiate directly towards the cold platen. Two electric heaters (Minco P/N HAP6948) provided a heat load to the SRDs, which allowed us to vary the temperature of the SRDs across the emissivity switching temperature.

### Experimental Apparatus and Test Methods

The test apparatus used to support the SRD plate in the TVAC chamber was designed and manufactured at the U of M. Figure 2 shows a CAD assembly of the test apparatus, with labels defining the naming convention of different components. The apparatus holds the SRD plate with the SRDs facing towards the radiation plate, which is in near-thermal equilibrium to the platen. We mounted the electric heaters on the top of the heater bracket, and placed insulating plastic spacers in joints

between components to minimize the thermal conductive paths.

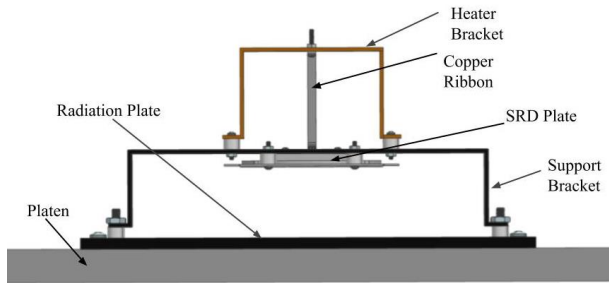


**Figure 2: Labelled diagram of test apparatus components.**

To emulate the heat path from the payload to the SRD plate, we used a tin-plated copper ribbon (5/8" wide and 1/16" thick) and a copper interface plate to provide a heat path from the heater bracket to the SRD plate. A 2 mm thick copper interface plate screwed into the existing heat pipe interface holes on the top side of the SRD plate, to increase the surface area where heat is applied to the SRD plate. The top edges of the ribbon screwed into the underside of the copper bracket, and the bottom face of the ribbon was a press fit against the copper interface plate. We inserted pieces of ChoTherm 1671 thermal gasket material between the copper ribbon and copper interface plate, as well as in the gaps between the heater bracket and the copper ribbon tab faces, in order to maximize heat transfer through the joint. Figure 3 shows a side view of the path of the copper ribbon from the heater bracket to the interface plate.

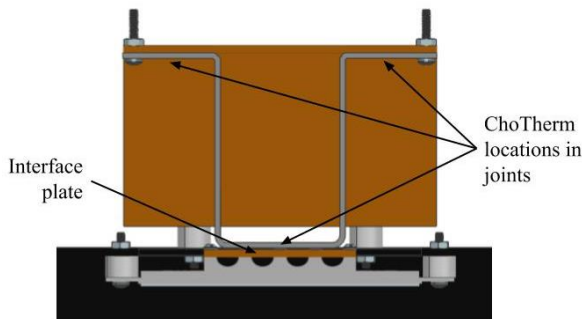


**Figure 3: CAD model side view of copper ribbon.**

The TVAC chamber does not have a cold shroud; therefore, in order to minimize parasitic heat loads from the room temperature ambient we installed an MLI blanket around the test apparatus. The MLI blanket consists of a 3 mm Kapton top layer followed by 9 layers of 1 mm aluminized Mylar, with netting between each layer for separation.

In order to measure the temperatures of the apparatus throughout the test, we instrumented the setup with 5kΩ thermistors from Omega (#44007). We installed the thermistors using beads of Stycast 2850 epoxy on top of pieces of copper tape. An Agilent data acquisition unit read the thermistor temperatures to a computer running Benchlink Data Logger software at a sampling rate of 0.1 Hz. We installed eight thermistors on the SRD plate. We installed no thermistors on the SRDs to prevent contamination and unrepresentative view factors. Instead, we installed four thermistors as close as possible to the SRDs on the edges of the plate where the SRDs are bonded. Figure 4 shows the location of these thermistors, as marked by stars. The area covered by the SRDs is marked with crosshatching for reference.

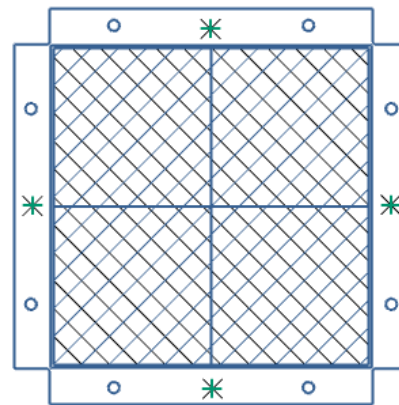


**Figure 4: Location of thermistors on SRD mounting side of SRD plate.**

We bonded an additional four thermistors on the opposite side of the plate, directly opposite (through the thickness of the plate) the area covered by the SRDs. Figure 5 shows the location of these thermistors, as marked by stars.

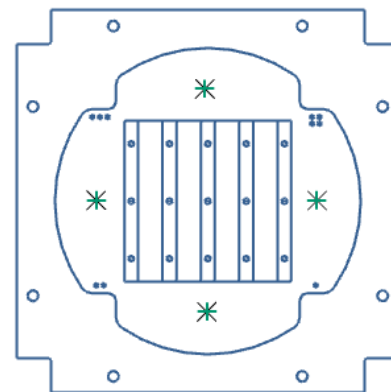


**Figure 5: Location of thermistors on heat pipe-interface side of SRD plate.**

Due to the low thermal capacity of the plate, we assumed the SRDs to be in thermal equilibrium with the plate edges for the ensuing analyses, and took the average of the four edge-mounted thermistors as the SRD temperature. The measured SRD temperature presented in the results section will be this calculated average.

We sealed the chamber and activated the pumps to reduce the chamber pressure to  $1 \times 10^{-3}$  torr or less. We recorded the actual chamber pressure at each steady state data point in the test procedure. Testing started with a cold soak of the entire test setup at the minimum platen temperature, and we then increased heater power at set increments and waited for the setup to stabilize. After reaching a defined equilibrium of  $1 \text{ }^\circ\text{C/hr}$ , we advanced to the next heater power setting.

### Results of Testing

Table 2 presents the results of the TVAC chamber testing for each heater input power setting. The SRD temperature in Table 2 is an average of the temperatures measured by the four thermistors on the SRD mounting side of the SRD plate. The platen temperature stated in the table is also an average, using five thermistors mounted on the cold surface the SRD plate radiated towards.

**Table 2: SRD Temperature Test Results**

Heater Power Input [W] (+/- 0.05)	Platen Temp. [ $^\circ\text{C}$ ] (+/- 0.2)	Chamber Pressure [torr] (+/- 0.05)	SRD Temp. [ $^\circ\text{C}$ ] (+/- 0.2)
0.00	-73.6	Not recorded	-62.7
1.03	-72.6	$1.5 \times 10^{-5}$	-54.0
2.54	-72.6	$1.2 \times 10^{-5}$	-40.5
6.43	-71.4	$9.1 \times 10^{-6}$	-9.9
9.69	-67.1	$9.7 \times 10^{-6}$	9.2
12.46	-64.8	$1.0 \times 10^{-5}$	20.3
14.90	-63.2	$1.0 \times 10^{-5}$	30.2
17.38	-61.9	$9.9 \times 10^{-6}$	39.8
19.84	-60.6	$9.5 \times 10^{-6}$	48.5
22.30	-59.1	$9.6 \times 10^{-6}$	56.6
24.74	-58.0	$1.0 \times 10^{-5}$	63.8
25.87	-56.7	$7.6 \times 10^{-6}$	67.0

### TEST DATA ANALYSIS AND DISCUSSION

After testing, we attempted to use the raw temperature data at each steady state point to calculate the emissivity profile of the SRDs. For these calculations, we considered the conductive heat paths through bolted joints, as well as the radiation terms for couplings we believed would be the largest contributors of radiative heat transfer (*i.e.*, face pairs with the highest view factors and the largest temperature difference).

Results of these calculations were inconclusive; we quickly realized that a number of unknown parameters in the calculations have a very large impact on the calculated emissivity profile of the SRDs. These variable parameters resulted in significant variations in the calculated emissivity values, at times resulting in illogical emissivity values (*i.e.*, outside of the expected range of emissivities of 0 to 1). These unknown parameters were mainly radiative view factors, neglected radiative couplings, and emissivities of surfaces. The following section describes these uncertainties in more detail.

### Sources of Uncertainty in Calculations

View factors were calculated where possible using equations from literature; for instance, for two parallel plates offset by a distance<sup>21</sup>. Where no equation from literature applied to a situation, we used NX Space Systems thermal to calculate an approximate view factor. The difficulty with this method is that it is not possible to verify the accuracy of the calculations by comparing the sum of the view factors to 1.0 (unity). For any radiation situation occurring in an enclosure, the sum of all view factors to other surfaces in the enclosure for a given surface should equal 1.0. Evaluating this view factor sum for a surface is a common method of checking the accuracy of view factor calculations<sup>22</sup>. However, since we were only considering a subset of the radiative couplings for these calculations, we could not use this verification method for our calculations.

The reason we did not consider all of the radiative couplings within the system in our calculations is due simply to the massive number of terms involved. Although there are not a large number of parts in the test apparatus, there are a large number of unique surfaces with view factors to multiple other surfaces, each requiring its own view factor calculated and radiative heat calculation performed. Even if we were to consider each of these radiative terms in our calculations, there would have been a significant amount of error associated with them due to the temperature variations across surfaces. The radiation equation assumes a constant temperature for a radiating surface, which is not always a reasonable assumption for this scenario given the relatively large temperature gradients across some surfaces (particularly the copper ribbon and the heater bracket).

The final major source of uncertainty in these calculations is the emissivity of some apparatus surfaces. We had the radiation plate and support bracket both black anodized in order to have more confidence in the emissivity of these surfaces; the side of the SRD plate with the SRDs attached was also black anodized (in the areas not covered by the SRDs). The reverse side of the

SRD plate, however, is machined aluminum. The emissivity of this surface is not as well defined as that of black anodize, with literature values ranging from 0.03 for buffed aluminum to 0.30 for heavily oxidized<sup>6</sup>. The more concerning unknown surface emissivity is that of the copper heater bracket and interface plate. Emissivity values for copper range from 0.03 for buffed copper to over 0.70 for heavily oxidized copper<sup>6,23</sup>. From the surface appearance of the copper in the test apparatus it was clear that a significant amount of oxidation had occurred, but the extent of this oxidation is difficult to quantify, creating uncertainty in the emissivity values. This emissivity has a relatively high impact on the calculated emissivity values, as there is a large radiative coupling between the copper heater bracket and the MLI surrounding the apparatus.

Due to the impact of these many sources of error, we were not able to calculate the emissivity profile of the SRDs using the methods intended for this article. However, all of these issues that we came across during our initial simplified analysis can be eliminated by using a thermal math model in thermal analysis software to simulate the testing situation. This type of analysis tool can easily calculate view factors for surfaces and take into account the temperature gradients across these surfaces by breaking each surface up into smaller elements to analyze. This kind of software tool will also allow us to determine the correct emissivity of the different surfaces by correlating temperature values at each plateau to the measured temperature data. Due to these reasons, developing and applying a thermal math model to this testing scenario will be the next step with this research.

### ***Practice Testing Lessons Learned***

Prior to the flight article testing which we presented here, we performed a number of practice tests using the same test apparatus, MLI blanket and thermistors, and using an Engineering Model (EM) of the SRD plate with a bare aluminum surface and no SRDs installed. We learned a number of important lessons from these practice tests, all of which contributed to improvements in our apparatus and methods leading to the final test on the flight article.

During our first practice test, we were seeing significant temperature gradients across parts that we expected to be relatively isothermal due to their small size and low thermal mass. Investigating this result, we realized that there were a number of areas of contact between the thermistor wires and different areas of the apparatus, creating conductive paths from areas of high temperature (*e.g.*, the SRD plate) to areas of low temperature (*e.g.*, the support bracket) that were having an impact on thermistor readings. For all follow-on tests we made sure to bundle wires and properly route bundles to prevent

this thermal bridging between different areas of the apparatus. In later practice tests, these unexpected temperature gradients reduced considerably and the measured temperatures of the SRD plate increased, implying that significant heat loss had resulted from these unintentional conductive paths.

A second concern with the thermistors that arose during practice tests was a lack of proper thermal contact between the thermistor bead and the surface being measured. For earlier testing, we adhered the thermistors to the apparatus by first applying a layer of Kapton tape for electrical isolation and then using a smaller piece of copper tape over top to adhere the thermistor bead and increase the thermal conductive path. However, we had concerns about the integrity and consistency of the thermistor bead to apparatus interface (*i.e.*, the possibility of thermistor peel-off). These concerns were partially due to the higher than expected temperature gradients mentioned in the previous paragraph, as well as visual inspection of the thermistors pre- and post-test. Therefore, we decided to semi-permanently bond the thermistors to the test apparatus (and SRD plate) using beads of thermal epoxy on top of a piece of copper tape in each measurement location. This method increased the contact area and conductive path between the thermistor bead and the measurement surface, and reduced the likelihood of thermistor movement during testing.

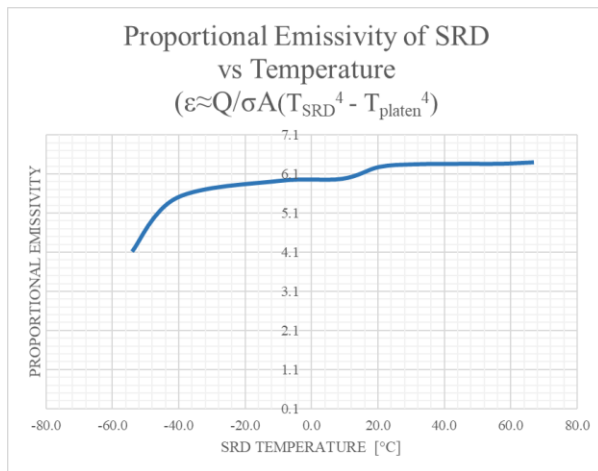
Comparisons between test data from the flight test and the practice tests also illustrated the large impact that inconsistent bolt torque has on the conductive path through joints as well as the time to stabilization for the apparatus. For the final flight article test we used a torque wrench when assembling the apparatus. The fasteners were much tighter than in previous tests and the system reached equilibrium much faster than for any of the practice tests (an average of two hours to stabilize rather than four). Given that the bolt torqueing was the largest difference from the previous test to flight testing, it is likely that the reason for this fast stabilization was the tighter / more consistent application of fasteners.

### ***General Trend in SRD Emissivity***

Although we cannot provide calculations of the exact emissivity profile of the SRDs at this point, we can still make conclusions about the general trend. The increases in SRD plate temperature using the flight hardware were less for this test than the increases in temperature that were seen for the same heater power increase during the practice testing with the EM plate. The EM plate had a constant emissivity (bare aluminum) surface radiating towards the cold radiation plate; this supports the expectation that the SRDs increase their emissivity with increasing temperature, as a smaller temperature increase indicates that the SRDs are operating as

expected. This is an extremely promising result, as this is the main aspect of this technology that allows it to provide improvements over traditional radiator materials.

We can also do some simple data manipulation to estimate the trend in SRD emissivity as temperature increases. If we rearrange Equation (1) for emissivity, we can use this expression with the SRD area ( $A$ ), SRD and platen temperatures ( $T_{SRD}$  and  $T_{platen}$ ), and heater power input ( $Q$ ), to calculate a very simplified proportional emissivity value. These calculated values are meant to be evaluated only in terms of the general trend, not for numerical values. Note that we assume that the trend in the radiated heat from the SRD plate is the same as the input heat from the heaters (which is a reasonable assumption given that this is the only change in inputs to the system from one state to the next). Given this assumption, the approximate trend for “proportional emissivity” versus SRD temperature shown in the following graph can be assumed to be representative of the SRD behavior.



As this graph shows, the emissivity of the SRDs is increasing with temperature. Future analyses using simulations with a thermal math model will enable higher accuracy in the value of  $Q$  to use in Equation (1) in order to provide better emissivity estimates.

## CONCLUSION

This paper presented TVAC test results of SRDs developed and manufactured by MPB, slated to fly on a Kepler Communications CubeSat. The SRDs radiated to a cold platen surface while we varied the SRD temperature using electrical heaters. During the test, we varied the temperature of the SRDs from  $-63^{\circ}\text{C}$  to  $+67^{\circ}\text{C}$  over 12 plateaus. Following testing, we attempted to evaluate the SRD emissivity at each plateau by calculating conductive and radiative thermal couplings

within the test apparatus. These calculations proved to be unreliable due to the uncertainty of several input parameters, as well as the complicated effects of the radiative heat transfer within the system proving to be beyond the computational limits of hand calculations.

Although we were not able to use the test data to directly calculate the emissivity profile of the SRDs in this article, there are still a number of valuable conclusions that can be made from this test. Firstly, our data shows that the SRDs are functioning as expected – the SRD emissivity clearly increases with temperature. A second major conclusion that we have made from this data is that thermal analysis of a TVAC test through a simplified control volume analysis of the test article is extremely error-prone, especially in the case of a small but complicated system such as this apparatus.

This second conclusion came as a surprise to the team who worked on this project, who are more familiar with thermal testing and analysis of much larger spacecraft and test articles. We have come to the realization that the difficulties in correlating the test data to simplified analytical equations are due largely to the extremely small size of the test article resulting in a much smaller signal to noise ratio than for analysis of a large spacecraft. Assumptions of constant temperature surfaces and approximations for view factor calculations are less valid at the small scale that we are considering, as the error introduced by these simplifications is no longer negligible for a test article of such small scale. This is an important conclusion to make about thermal testing in a vacuum environment, which has direct implications for thermal testing of small satellites.

Due to the identified difficulties with hand calculations, we believe that the only way analyze the test data accurately will be through finite element simulations of the test conditions using a thermal analysis software, such as NX Space Systems Thermal. We will develop a thermal math model of the test apparatus and correlate the model to the raw temperature data we have collected, in order to infer the values of SRD emissivity at each plateau. Performing these simulations in order to more accurately characterize the emissivity profile of the SRDs will be the next step in this research.

## REFERENCES

1. R. Osiander, S. L. Firebaugh, J. L. Champion, D. Farrar and M. A. G. Darrin, "Microelectromechanical Devices for Satellite Thermal Control," IEEE Sensors Journal, vol. 4, no. 4, pp. 525-531, 2004.

2. D. G. Gilmore, *Spacecraft Thermal Control Handbook: Fundamental technologies*, El Segundo: The Aerospace Press, 2002.
3. C. Carlisle and E. H. Webb, "Space Technology 5 - A Successful Micro-Satellite Constellation Mission," in *21st Annual AIAA/USU Conference on Small Satellites*, Logan, 2007.
4. E. Haddad, R. V. Kruzelecky, B. Wong, W. Jamroz, A. Hendaoui, M. Chaker and P. Poinas, "Large Tuneability IR Emittance Thermal Control Coating for Space Applications," in *43rd International Conference on Environmental Systems*, Vail, CO, 2013.
5. H. Brouwer and Z. D. Groot, "Solving the Thermal Challenge in Power-Dense CubeSats with Water Heat Pipes," in *31st Annual AIAA/USU Conference on Small Satellites*, Logan, UT, 2017.
6. E. Haddad, M. Benkahoul, R. V. Kruzelecky, B. Wong, W. Jamroz, M. Soltani, A. Hendaoui, M. Chaker and P. Poinas, "Monitoring thermo-optical properties of Multilayer Tuneable Emittance Coatings for Smart Thermal Control in Space," in *41st International Conference on Environmental Systems*, Portland, OR, 2011.
7. S. Janson, "25 Years of Small Satellites," in *25th Annual AIAA/USU Conference on Small Satellites*, Logan, Utah, 2011.
8. L. S. Novikov, V. N. Mileev, E. N. Voronina, L. I. Galanina, A. A. Makletsov and V. V. Sinolits, "Radiation Effects on Spacecraft Materials," *Journal of Surface Investigation. X-ray, Synchrotron and Neutron Techniques*, vol. 3, no. 2, p. 32–48, 2009.
9. Y. Zhu, L. Guo, J. Qiao and W. Li, "An enhanced anti-disturbance attitude control law for flexible spacecrafts," *Control Engineering Practice*, vol. 84, p. 274–283, 2019.
10. D. Pignatelli, R. Nugent and J. Puig-Suari, "Improving Launch Vibration Environments for CubeSats," in *31st Annual AIAA/USU Conference on Small Satellites*, Logan, Utah, 2017.
11. M. R. Reddy, "Effect of low earth orbit atomic oxygen on spacecraft materials," *Journal of Materials Science*, vol. 30, pp. 281-307, 1995.
12. T. Bohnke, H. Kratz, A. Hultaker, J. Kohler, M. Edof, A. Roos, C.-G. Ribbing and G. Thornell, "Surfaces with high solar reflectance and high thermal emittance on structured silicon for spacecraft thermal control," *Optical Materials*, vol. 30, p. 1410–1421, 2008.
13. A. J. Juhasz and G. P. Peterson, "Review of Advanced Radiator technologies for spacecraft thermal control," *National Aeronautics and Space Administration*, Cleveland, 1994.
14. T. Miyakita, R. Hatakenaka and H. Sugita, "Evaluation of Thermal Insulation Performance of a New Multi-Layer Insulation with Non-Interlayer-Contact Spacer," in *45th International Conference on Environmental Systems*, Bellevue, Washington, 2015.
15. T. D. Swanson and G. C. Birur, "NASA thermal control technologies for robotic spacecraft," *Applied Thermal Engineering*, vol. 23, p. 1055–1065, 2003.
16. S. A. Budnik, A. N. Nenarokomov and D. M. Titov, "Investigation of Passive Systems for Thermal Control of Spacecraft," *Journal of Engineering Physics and Thermophysics*, vol. 91, no. 6, pp. 1565-1572, 2018.
17. J. Currano, S. Moghaddam, J. Lawler and K. Jungho, "Performance Analysis of Electrostatic Switched Radiator Using Heat-Flux-Based Emissivity Measurement," *Journal of Thermophysics and Heat Transfer*, vol. 22, no. 3, pp. 360-366, 2008.
18. W. R. Wade, "Measurements of Total Hemispherical Emissivity of Various Oxidized Metals at High Temperatures," *National Advisory Committee for Aeronautics*, Langley Field, Va., 1958.
19. K. B. Narayana, "View Factors for Parallel Rectangular Plates," *Heat Transfer Engineering*, vol. 19, no. 1, pp. 59-63, 1997.
20. G. Salazar, J. C. Droba, B. Oliver and A. J. Amar, "Development and Verification of Enclosure Radiation Capabilities in the CHarring Ablator Response (CHAR) Code," in *46th AIAA Thermophysics Conference*, Washington, D.C., 2016.
21. N. L. Johnson, "Orbital Debris: The Growing Threat to Space Operations," *Advances in the Astronautical Sciences*, vol. 137, pp. 3-11, 2010.
22. A. Hendaoui, N. Émond, S. Dorval, M. Chaker and E. Haddad, "VO2-based smart coatings with improved emittance-switching properties for an

energy-efficient near room-temperature thermal control of spacecrafts," *Solar Energy Materials & Solar Cells*, vol. 117, pp. 494-498, 2013.

23. T. Kim, S.-H. Han and H.-U. Oh, "Design and Performance Evaluation of MEMS-Based Spaceborne Variable Emissivity Radiator Using Movement of Electrified Beads," *Journal of Microelectromechanical Systems*, vol. 26, no. 1, pp. 113-119, 2017.